Carbohydrate Polymers 102 (2014) 790–798

Contents lists available at ScienceDirect

Carbohydrate Polymers

journal homepage: www.elsevier.com/locate/carbpol

Modification of tapioca starch by non-chemical route using jet atmospheric argon plasma

Rungtiwa Wongsagonsup[a], Panakamol Deeyai[b], Weerawut Chaiwat[c], Sawanee Horrungsiwat[a], Kesini Leejariensuk[a], Manop Suphantharika[d], Asira Fuongfuchat[e], Somsak Dangtip[f,g,*]

[a] Food Technology Program, Mahidol University, Kanchanaburi Campus, Kanchanaburi 71150, Thailand
[b] Materials Science and Engineering Program, Faculty of Science, Mahidol University, Bangkok 10400, Thailand
[c] Environmental Engineering and Disasters Management Program, Mahidol University, Kanchanaburi Campus, Kanchanaburi 71150, Thailand
[d] Department of Biotechnology, Faculty of Science, Mahidol University, Bangkok 10400, Thailand
[e] National Metal and Materials Technology Center (MTEC), National Science and Technology Development Agency (NSTDA), Ministry of Science and Technology, Klong Luang, Pathum Thani 12120, Thailand
[f] Department of Physics and NANOTEC CoE at Mahidol University, Faculty of Science, Mahidol University, Bangkok 10400, Thailand
[g] ThEP Center, CHE, Ministry of Education, Bangkok 10400, Thailand

ARTICLE INFO

Article history:
Received 24 May 2013
Received in revised form 21 October 2013
Accepted 29 October 2013
Available online 6 November 2013

Keywords:
Modified tapioca starch
Jet atmospheric argon plasma
Rheological properties
Structural characteristics
Cross-linking
Depolymerization

ABSTRACT

Non-chemical modification of tapioca starch was investigated using jet atmospheric argon plasma treatment. Two forms of starch slurry, i.e. granular starch (G) and cooked starch (C), were jet-treated by argon plasma generated by supplying input power of 50 W (denoted as G50 and C50 samples) and 100 W (denoted as G100 and C100 samples) for 5 min. Physical, rheological, and structural characteristics of the modified starch were investigated. The G50 and C100 samples had lower paste clarity but higher thermal stability and performed stronger gels (G50 only) compared to their control counterparts. On the other hand, the analyzed properties of the G100 and C50 samples showed the opposite trend. FTIR and ^{1}H NMR results revealed that the relative areas of C—O—C and OH peaks were changed after the treatment. Cross-linking reaction seemed to predominantly take place for the G50 and C100 samples, whereas depolymerization predominated for the G100 and C50 samples.

© 2013 Elsevier Ltd. All rights reserved.

1. Introduction

Tapioca is one of the most important industrial crops in Thailand. Tapioca starch, obtained from cassava root processing, is used for a wide range of applications including foods and non-foods. The physical characteristics of tapioca starch paste are odorless, high clarity and high stickiness. However, the native starch paste has some shortcomings in food applications such as unstable viscosity to heat, acid and shear forces, weak structure and undesirable gel characteristic. These drawbacks could be overcome by starch modification including physical and chemical methods. Chemical methods typically give high efficiency in starch modification but their disadvantages are concerned in points of food safety, and cost of chemicals and waste water treatment. In the contrary, physical methods could overcome the shortcomings of chemical modifications due to no chemical residues, and cost reduction in chemicals and waste water treatment.

Among the physical modification methods, plasma treatment is recognized as one of novel methods to the area of starch modifications (Deeyai, Jitsomboonmit, Soonthonchaikul, Suphantharika, & Dangtip, 2010; Deeyai, Suphantharika, Wongsagonsup, & Dangtip, 2013). Plasma is an ionized gas consisting of various types of highly active species, e.g. electrons, ions, excited atoms and photons (Bogaerts, Neyts, Gijbels, & Van der Mullen, 2002; Raizer, 1991). The plasma is induced when supplying enough energy to gas under suitable conditions. For applications in starch modifications, the plasma treatments were mostly conducted under vacuum of which pressure was far below atmospheric pressure (Lii, Liao, Stobinski, & Tomasik, 2002a, 2002b, 2002c; Pashkuleva, Marques, Vaz, & Reis, 2010; Szymanowski, Kaczmarek, Gazicki-Lipman, Klimek, & Woźniak, 2005; Zou, Liu, & Eliasson, 2004). In such treatments, several gases, such as ethylene, hydrogen, oxygen, ammonia, air, methane, argon and so on, were utilized as plasma source. These treatments were able to modify starch in different aspects

* Corresponding author at: Department of Physics and NANOTEC CoE at Mahidol University, Faculty of Science, Mahidol University, Bangkok 10400, Thailand. Tel.: +66 2201 5852; fax: +66 2201 5843.
E-mail address: somsak.dan@mahidol.ac.th (S. Dangtip).

0144-8617/$ – see front matter © 2013 Elsevier Ltd. All rights reserved.
http://dx.doi.org/10.1016/j.carbpol.2013.10.089

depending on plasma types and conditions used. The modifications were, for examples, increase in surface energy, increase or decrease in hydrophilicity, oxidation, bond breaking or depolymerization, and cross-linking. Nevertheless, stable glow discharge plasma of air, argon, oxygen and nitrogen was reported to be able to conduct at atmospheric pressure using a source operating at 50 Hz (Okazaki, Kogoma, Uehara, & Kimura, 1993).

Recently, the utilization of dielectric barrier discharge (DBD) argon plasma at atmospheric pressure on starch modifications has been explored by Deeyai et al. (2010, 2013) and found that cross-linking reaction took place in tapioca starch especially under low relative humidity. Dealing with atmospheric pressure condition could be easy for handling and economical in terms of energy usage. However, starch was prepared in thin tablet form or thin layer before treating under DBD atmospheric argon plasma because the possible gap between two electrodes was just a few mm (Deeyai et al., 2010, 2013). Also, only starch granules on the surface of the tablet can be exposed to plasma. Applying jet argon plasma could lend further flexibility to DBD plasma, namely, being able to treat starch in other forms, for example, slurry, thus allows the starch sample to be treated more thoroughly.

At present, however, to the best of our knowledge, there is no research on the modification of starch using jet argon plasma at atmospheric pressure. Thus, the objectives of this research were to modify tapioca starch using jet atmospheric argon plasma, to determine physical and rheological properties and characterize functional structures of the modified starch; and finally to propose the possible mechanisms following jet argon plasma treatment under atmospheric pressure. Two forms of starch slurry, i.e. granular starch (intact granules) and cooked starch (well dispersed suspension), were used in this study in order to investigate effects of the slurry form on type of reaction and reaction pattern occurring during the treatment.

2. Materials and methods

2.1. Materials

Tapioca starch was kindly provided by Siam Modified Starch Co. Ltd. (Pathum Thani, Thailand). Potassium thiocyanate (KSCN) (Ajax Finechem Pty Ltd., Taren Point, Australia) for FTIR analysis and dimethyl sulfoxide-d_6 (DMSO-d_6) (Cambridge Isotope Laboratories, Inc., Andover, MA) for ^{1}H NMR analysis were of analytical grade.

2.2. Sample preparation for jet argon plasma treatment

Two forms of starch slurry were prepared as granular and cooked starch. For granular starch, 0.4 g of starch was dispersed in 1.6 g of distilled water to obtain a starch concentration of 20% (w/w). The slurry was thoroughly mixed using a magnetic stirrer. For cooked starch, 0.1 g of starch was dispersed in 4.9 g of distilled water to obtain a concentration of 2% (w/w), the slurry was then boiled for 2 min with stirring. The cooked starch was cooled to room temperature (25 °C) for 7 min before subjecting to plasma treatment.

2.3. Jet argon plasma treatment under atmospheric pressure

The schematic diagram of jet atmospheric argon plasma setup is shown in Fig. 1. Argon plasma was induced by supplying sufficient input power and high frequency (HF) to argon gas under atmospheric pressure. In this study, the input power supplied for generating plasma was 50 or 100 W. The HF of power supply was about 600 MHz. The starch slurry was treated by jet argon plasma for 5 min. During the treatment, slurries of both granular and cooked starch were continuously stirred using a magnetic stirrer to prevent sedimentation.

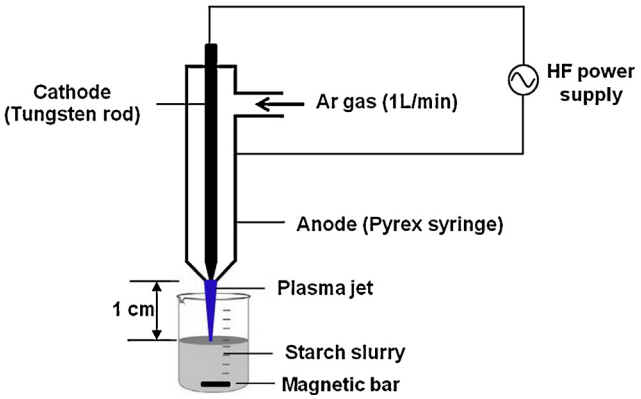

Fig. 1. Schematic diagram of jet atmospheric argon plasma set up.

2.4. Handling of sample after plasma treatment

After the treatment, the plasma-treated starch was centrifuged and dried at 40 °C overnight. Absolute ethanol was used to precipitate cooked starch sample before centrifugation. The dried samples were kept in a chamber containing saturated $Mg(NO_3)_2$ with 50% relative humidity to equilibrate moisture content of all samples.

2.5. Starch paste clarity determination

Clarity of starch paste was determined by measuring light transmittance according to the modified method of Craig, Maningat, Seib, and Hoseney (1989). Starch paste solution (1%, w/v) was prepared by suspending 0.25 g starch in 25 mL distilled water in a 50-mL centrifuge tube and then placed in a boiling water bath for 30 min with mild stirring. After cooling to room temperature for 10 min, the percentage of light transmittance (%T) at 650 nm was determined against distilled water using a double-beam UV–vis spectrophotometer (UV 1800, Shimadzu Corporation, Kyoto, Japan).

2.6. Thermogravimetry analysis

Thermogravimetry analysis was performed using a thermogravimetric analyzer (TGA) (Mettler-Toledo AG, Schwerzenbach, Switzerland). Starch powder sample was heated from 25 °C to 500 °C at a heating rate of 10 °C/min in a nitrogen stream. Percent weight loss was calculated by the percent weight difference between 270 °C and 350 °C (Lii et al., 2002b, 2002c).

2.7. Differential scanning calorimetry analysis

Sample was mixed with distilled water at a ratio of 1:3 (w/w), hermetically sealed in an aluminum pan, and then equilibrated at room temperature for 1 h. The sample was heated from 25 °C to 100 °C at a heating rate of 10 °C/min using a differential scanning calorimeter (DSC) (DSC-1 STAR^e System, Mettler-Toledo AG, Schwerzenbach, Switzerland). A sealed empty pan was used as a reference. Onset (T_o), peak (T_p), and conclusion (T_c) gelatinization temperatures and enthalpy change (ΔH) of gelatinization of starch were recorded.

2.8. Microscopic observation

In order to investigate the relationship between rheological properties and microscopic structures of starch dispersions, all

Table 1
Light transmittance (%*T* at 650 nm) of the plasma-treated granular and cooked starch paste solutions (1%, w/v) and DSC thermal properties of the plasma-treated granular starch compared with those of the untreated starch samples.[a]

Sample	Light transmittance		DSC thermal properties[b]			
	Granular starch	Cooked starch	T_o (°C)	T_p (°C)	T_c (°C)	ΔH (J/g)
Untreated	34.9 ± 0.1b	75.0 ± 0.1b	64.0 ± 0.1a	70.2 ± 0.1a	79.1 ± 0.1a	14.2 ± 1.0ab
50-W-treated	32.6 ± 0.1c	78.2 ± 1.7a	64.4 ± 0.5a	70.4 ± 0.5a	79.6 ± 0.8a	14.9 ± 0.6a
100-W-treated	39.5 ± 0.9a	72.8 ± 1.1c	64.1 ± 0.3a	70.4 ± 0.5a	79.0 ± 0.4a	13.0 ± 0.2b

[a] Mean ± standard deviation values in the same column with different letters are significantly different ($P < 0.05$).
[b] T_o, T_p, and T_c are the onset, peak, and conclusion gelatinization temperatures, respectively. ΔH is the gelatinization enthalpy.

starch pastes prepared for rheological analysis were observed under an optical microscope (Olympus BX51, Olympus Optical Co. Ltd., Tokyo, Japan) with iodine (0.2%, w/v) staining.

2.9. Rheological analysis

Starch pastes (6%, w/w) were prepared by heating starch suspensions in a boiling water bath for 20 min. After cooling to room temperature (~10 min), the pastes were subjected to rheological analysis. Dynamic viscoelastic property and steady flow behavior of the sample were determined at 25 °C using a rotational rheometer (Gemini 200 HR Nano, Malvern-Bohlin Instruments, Worcestershire, UK) with a cone and plate geometry (titanium cone with 1° cone angle, 40 mm diameter, and 0.07 mm gap). Before each measurement, the sample was pre-sheared at a shear rate of 0.01 s^{-1} for 10 s and equilibrated for 10 s. The frequency sweep range was 0.1–100 rad s^{-1} with controlled stress at 1 Pa for granular starch samples and 0.3 Pa for cooked starch samples, which were in the linear viscoelastic region (LVR). The degree of frequency dependence was determined by power law parameters as:

$$G' = A\omega^B \quad (1)$$

where G' is the storage modulus (Pa), ω is the oscillation frequency (rad s^{-1}), and A and B are the constants (Khondkar, Tester, Hudson, Karkalas, & Morrow, 2007; Yoneya, Ishibashi, Hironaka, & Yamanoto, 2003).

After oscillatory test was completed, the sample was subjected to steady flow measurement. The cone was programmed to ramp up and down in 2 cycles with shear rates of 1–300 s^{-1} for 300 s in each cycle. The data of shear stress and shear rate of shear ramping up of the second cycle was used to characterize flow behavior of the sample and to estimate the power law parameters by using the following equation:

$$\sigma = K\dot{\gamma}^n \quad (2)$$

where σ is the shear stress (Pa), $\dot{\gamma}$ is the shear rate (s^{-1}), K is the consistency coefficient (Pa s^n), and n is the flow behavior index (dimensionless).

2.10. Fourier transform infrared (FTIR) spectroscopy measurement

FTIR spectra were recorded (64 scans with a spectral resolution of 4 cm^{-1}) in attenuated total reflection (ATR) mode on a Nicolet 6700 FTIR spectrometer (Thermo Electron Corporation, Madison, WI, USA). The detector was cooled with liquid nitrogen before collecting spectra for at least 20 min. The absorbance spectra were computed between 4000 and 400 cm^{-1}. The sample spectra were recorded against a background spectrum which was a spectrum without sample in place. All measurements were analyzed using OMNIC software. Quantitative measurement of specific functional group in structure of starch molecules was performed using an internal standard FTIR technique (Davis, Erickson, Johnston, Delfino, & Porter, 1999). Potassium thiocyanate (KSCN) was chosen as an internal standard. The spectral data were baseline corrected and normalized against the KSCN internal standard peak at 2050 cm^{-1}.

2.11. Proton nuclear magnetic resonance (^{1}H NMR) measurement

The starch samples were dissolved in dimethyl sulfoxide-d_6 (DMSO-d_6). At first, 0.2 g of starch powder was dissolved in 1 mL DMSO-d_6. The solution was then stirred for 10 min before keeping in an oven at 80 °C for two days to completely solubilize starch molecules (Liu, Chaudhary, Yusa, & Tadé, 2011). The ^{1}H NMR spectra of the starch samples were obtained using a Bruker DPX 300 NMR spectrometer at 300 MHz (Germany). The NMR data was collected for 100 scans to obtain good spectra. The chemical shift of DMSO-d_6 was calibrated at 2.49 ppm (Dragunski & Pawlicka, 2001; Zou et al., 2004). The peak of H-4, H-5 (chemical shift of 4.5 ppm) assigned to α-D glucose was considerably stable, indicating that it was unaffected by the plasma modification. Thus, the H-4, H-5 peak was performed as an internal standard (Zou et al., 2004). The peak found at 5.0 ppm was corresponded to the hydroxyl groups (R-OH) (Cheng & Neiss, 2012; Dragunski & Pawlicka, 2001). The relative area of hydroxyl group in each spectrum to the area of H-4, H-5 peak was calculated.

2.12. Statistical analysis

Experimental data were analyzed using SPSS statistical software version 13.0 (SPSS Inc., Chicago, IL, USA). Analysis of variance (ANOVA) was performed using Duncan's multiple range test to compare mean values. Significant difference was defined at $P < 0.05$.

3. Results and discussion

3.1. Starch paste clarity

The possible main reactions occurred during plasma treatment can be cross-linking and depolymerization (Lii et al., 2002a, 2002b, 2002c; Zou et al., 2004), depending on plasma type and set-up condition, which alter the physicochemical properties of native starch. The cooked starch slurry encountered the cooking process twice, i.e. during sample preparation for plasma treatment and paste clarity analysis, resulting in almost complete dispersion with few of small aggregates, and thus exhibited higher clarity than its granular starch slurry counterpart (Table 1). It has been reported that the light transmittance value of pre-gelatinized cold-water-soluble starch was higher than that of the native one (Bello-Pérez, Romero-Manilla, & Paredes-López, 2000). The 50 W plasma-treated granular starch (G50) and the 100 W plasma-treated cooked starch (C100) had significantly lower paste clarity than their untreated counterparts (Table 1), probably due to the predominant effect of cross-linking reaction occurred during the plasma treatment. Cross-linking of starch has been reported to reduce clarity or light transmittance of starch paste (Craig et al., 1989; Jyothi, Moorthy, & Rajasekharan, 2006; Kaur, Singh, & Singh, 2006; Kerr & Cleveland,

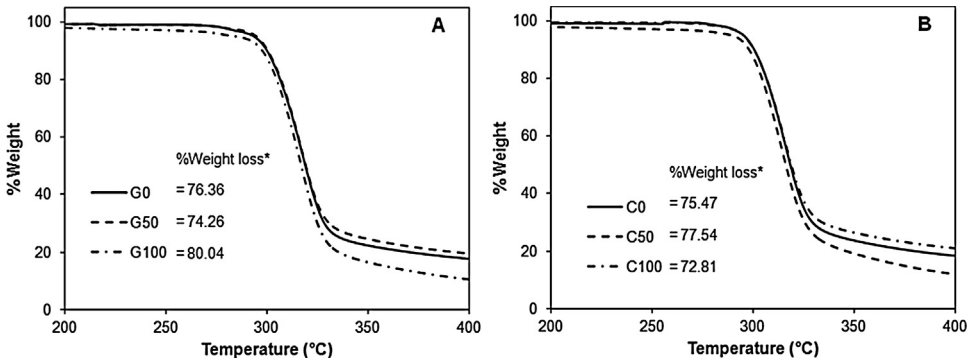

Fig. 2. TGA thermograms and %weight loss of the untreated starches (G0 and C0) and plasma-treated starches at 50 W (G50 and C50) and 100 W (G100 and C100). A: granular starch (G), B: cooked starch (C). *%Weight loss = %weight at 270 °C − %weight at 350 °C.

1959; Koo, Lee, & Lee, 2010; Reddy & Seib, 2000). Lim and Seib (1993) proposed that determination of light transmittance of chemically phosphorylated starch pastes can be an alternative test to determine the extent of cross-linking of starch. Cross-linking prevents starch chains from dissociation, thus cross-linked starch paste has more entanglement structure than the native starch one, resulting in a decreased paste clarity. On the other hand, the light transmittance values of the 100 W plasma-treated granular starch (G100) and the 50 W plasma-treated cooked starch (C50) were significantly higher than those of their control counterparts (Table 1), which might signify the preference of the depolymerization effect to the cross-linking one. The shorter or smaller starch molecules dispersed and solubilized easily during gelatinization, leading to the more dissociated starch molecules, which facilitate improved paste clarity. It is well recognized that depolymerization of starch by chemical modification such as acid thinning causes an increase in light transmittance of acid-thinned starch pastes compared to those of the native ones (Dutta, Paul, Kalita, & Mahanta, 2011; Lawal, 2004; Sandhu, Singh, & Lim, 2007). The increased light transmittance of acid-thinned starch paste is due to its decreased retrogradation tendency (Sandhu et al., 2007).

3.2. Thermogravimetric analysis

Thermogravimetric results showed that weight losses of the G50 and C100 samples were less than those of their native counterparts during heat treatment (Fig. 2). On the other hand, the G100 and C50 samples showed the opposite trend, i.e. weight losses were increased after plasma treatment, indicating their relatively weaker structure. It means that the G50 and C100 samples had more thermal stability and relatively stronger structure after plasma treatment, which might be due to the predominant occurrence of cross-linking reaction during plasma treatment. Singh and Nath (2012) reported that cross-linked sago starch exhibited more thermal stability as compared to native sago starch. Thus, the causes of their relatively weaker structures of the G100 and C50 might come from the higher profound depolymerization effect. These results are in good agreement with those reported by Lii et al. (2002b, 2002c), who described that depolymerized starches obtained from low pressure ammonia, hydrogen, oxygen, and ethylene plasma treatment exhibited an increase in weight loss compared to the native ones.

3.3. Differential scanning calorimetry (DSC)

As DSC analysis was performed to determine gelatinization characteristics of starch, therefore this technique cannot be applied for analysis of the cooked starch samples. Thermal properties of untreated and plasma-treated granular starch samples by DSC analysis are shown in Table 1. Gelatinization temperatures, i.e. T_o, T_p, and T_c, of all treated samples were not significantly different from those of the untreated one. However, ΔH of the G50 sample was slightly higher than that of the control, but significantly higher than that of the G100 sample. It has been reported that the ΔH of starch increased with increasing level of cross-linking while gelatinization temperature was not affected by cross-linking (Choi & Kerr, 2004; Yeh & Yeh, 1993). Jyothi et al. (2006) found that ΔH of cross-linked starch increased with increasing degree of cross-linking, but the gelatinization temperatures slightly reduced after cross-linking. The cross-linking reaction retains the integrity of starch granules, thus more heat or energy was needed for gelatinization (Rutenberg & Solarek, 1984). The ΔH reflects mainly the loss of double helical structure rather than crystalline order, higher ΔH indicates higher granule stability (Cooke & Gidley, 1992). In contrast, cross-linking of banana starch with STMP/STPP and EPI exhibited an increase in gelatinization temperatures, but a slight decrease in ΔH (Carmona-Garcia, Sanchez-Rivera, Méndez-Montealvo, Garza-Montoya, & Bello-Pérez, 2009). The ΔH of cross-linked potato starch was varied (either decreased or increased) depending on the concentration of $POCl_3$ used in the reaction (Yoneya et al., 2003). Chatakanonda, Varavinit, and Chinachoti (2000) reported that ΔH was not affected by cross-linking. Therefore, according to earlier reports, the effect of cross-linking on gelatinization properties has been found to depend on the nature of the starch source and the cross-linking conditions used. In case of depolymerization effect, the obtained results are consistent with those of López, Zaritzky, and García (2010), who reported that depolymerized corn starch by acid modification showed unchanged gelatinization temperatures, while its ΔH was lower than that of the native one. The ΔH of acid-thinned normal and waxy corn starches decreased as compared to those of their native counterparts (Sandhu et al., 2007). Some degree of amorphous regions might be lost during acid treatment.

3.4. Microscopic observation

Prior to rheological testing, the morphological structure of starch paste was observed under an optical microscope in order to determine structure–rheology relationship. There was no swollen granule remained in the paste for all samples. The granules were mostly disintegrated and only a few degraded granule remnants were observed in the case of G samples (data not shown). The untreated cooked starch (C0) had completely dissolved after gelatinization (Fig. 3A). The plasma treatment at 50 W (C50) and 100 W (C100) induced formation of undissolved, highly cross-linked clusters of starch molecules as shown in Fig. 3B and C, respectively. In the cooked starch sample, most of the starch molecules dispersed freely. When one point of cross-linking occurred during

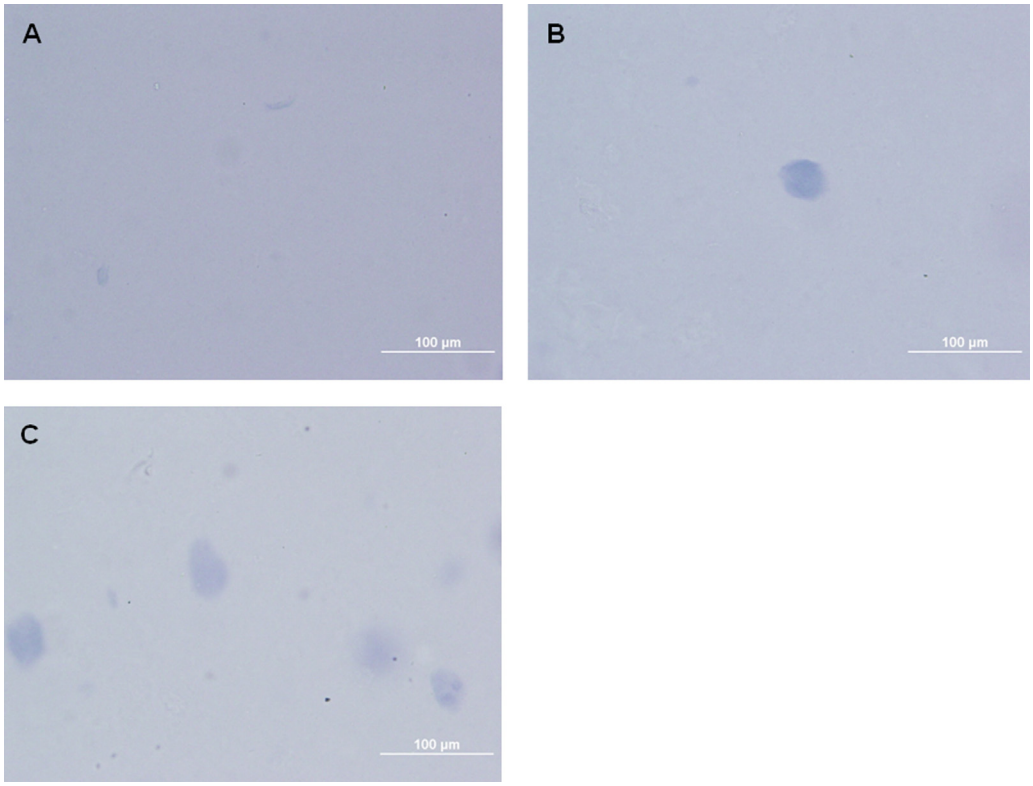

Fig. 3. Optical micrographs of iodine-stained pastes (6%, w/w) of the untreated and plasma-treated cooked starches: (A) C0, (B) C50, and (C) C100.

plasma treatment, it can contribute other cross-linking points to be occurred in the adjacent starch chains, resulting in the undissolved, highly cross-linked clusters. The cross-linking was more pronounced for the C100 sample than the C50 sample as evidenced by a higher number of cross-linked clusters observed in Fig. 3C than in B. Consequently, starch concentration in a continuous phase of the C100 sample was substantially diluted.

3.5. Rheological properties

For dynamic viscoelastic properties, the magnitudes of elastic behavior, storage modulus (G'), and viscous behavior, loss modulus (G''), plotted as a function of angular frequency can provide information on gel structure. The magnitude of G' of all G samples was slightly higher than that of the G'' along the frequency range tested (Fig. 4A and B) and both G' and G'' were frequency-dependent (the constant $B > 0$ in Table 2), indicating that all G paste samples had soft gel behavior. Moreover, the G50 paste exhibited a lower magnitude of loss tangent ($\tan\delta$), i.e. a value of G''/G', than the control one (G0) (Fig. 4C), indicating that the G50 paste had stronger gel structure than the G0, presumably due to an enhancement by cross-linking reaction. In contrast, the G100 paste exhibited lower magnitudes of both G' and G'' and higher values of $\tan\delta$ than the G0 paste, indicating a weakening of gel structure of the G100 sample possibly caused by the depolymerization effect of plasma treatment. Khondkar et al. (2007) found that G' and complex viscosity (η^*) of cross-linked starch were higher than those of native starch. It was also reported that cross-linked potato starch with $POCl_3$ had lower $\tan\delta$ than the control one (Yoneya et al., 2003). In general, an increase of G' accompanied with a decrease of $\tan\delta$ suggests a formation of polymer cross-linking (Yoneya et al., 2003). Therefore, the enhanced network observed in the G50 possibly due to the permanent cross-link junctions presented in the sample.

Table 2
Power law constants for relationships between storage modulus and frequency ($G' = A\omega^B$) and between shear stress and shear rate ($\sigma = K\dot{\gamma}^n$) of the untreated and plasma-treated starch pastes (6%, w/w).

Sample[a]	Dynamic viscoelastic test			Steady flow test		
	A (Pa s)	B (slope)	R^2	K (Pa s^n)	n (−)	R^2
G0	3.97	0.43	0.990	11.21	0.52	0.998
G50	5.08	0.38	0.981	11.43	0.49	0.996
G100	3.19	0.46	0.985	9.68	0.50	0.997
C0	NA[b]	NA	NA	5.58	0.43	0.999
C50	NA	NA	NA	2.28	0.42	1.000
C100	NA	NA	NA	1.60	0.38	1.000

[a] G0, untreated granular starch; G50, plasma-treated granular starch at 50 W; G100, plasma-treated granular starch at 100 W; C0, untreated cooked starch; C50, plasma-treated cooked starch at 50 W; C100, plasma-treated cooked starch at 100 W.
[b] NA: not analyzed.

Power law parameters calculated from the results of both oscillatory (Eq. (1)) and steady shear tests (Eq. (2)) of all samples are shown in Table 2. For dynamic viscoelastic properties, it is known that $B = 0$ for a covalent gel, while $B > 0$ for a physical gel. The B value is related to the strength and mature of the gel (Khondkar et al., 2007; Yoneya et al., 2003). Higher the B value, weaker the gel obtained. Thus, the strength of gel can be ordered as G50 > G0 > G100 for G samples. Khondkar et al. (2007) reported that the higher B value of uncross-linked starch indicating that the gel of native starch was not as strong as the gel of cross-linked starch.

For steady flow test, the G0 displayed a combined hysteresis loop, i.e. a small clockwise loop at high shear rates and a counter-clockwise loop at low shear rates (data not shown), indicating both thixotropic and anti-thixotropic behaviors, respectively, in the first cycle of shear ramping. The data of shear ramping of the second cycle, however, was almost identical to that of the shear ramping down of the first cycle and showed non-thixotropic behavior.

Moreover, the G50 and G100 samples displayed no hysteresis loop. Therefore, in this study, the data of shear stress and shear rate of the shear ramping up of the second cycle was used to characterize the flow behavior of the samples using power law equation. It was found that the G50 paste exhibited the highest consistency coefficient (K) following by the G0 and G100, respectively (Table 2).

From the rheological results of the G samples, it can be concluded that the G50 paste had the highest in both consistency and modulus, indicating the stronger gel and the presence of permanent cross-link junctions. The G100, however, had the lowest consistency and modulus. A weaker structure observed in the G100 may thus be attributed to the depolymerized species in the sample.

For the cooked starch (C) samples, the dynamic viscoelastic properties of the C samples were quite different from those of the G samples. All C samples exhibited $G'' > G'$ with a cross-over at high frequencies (Fig. 4D and E), indicating the most liquid-like behavior. The starch paste was very thin since it encountered heating process twice, i.e. during sample preparation for plasma treatment and rheological test. The more completely dissolved paste with some starch remnants in the continuous phase made the smaller G' value. Because of the liquid-like behavior of the C samples, the power law constants of viscoelastic test, which is applicable to gel samples, was not either analyzed or used for discussion. The plots of G', G'', and tan δ as a function of angular frequency (Fig. 4D–F, respectively) were then used in the discussion of this case. Overall features showed that magnitudes of both G' and G'' at low frequencies were ordered as C0 > C50 > C100. The predominant effect of starch depolymerization in the case of C50 sample could lower its modulus compared to that of the control (C0). In the case of the C100 sample, dominant cross-linking was proposed. The modulus values of the C100 sample were, however, lower (Fig. 4D and E) and accompanied by higher tan δ values (Fig. 4F) than those of both the C0 and C50 samples, due to the substantially low starch concentration in the continuous phase with numbers of undissolved starch clusters of highly cross-linked areas as observed by an optical microscope (Fig. 3C).

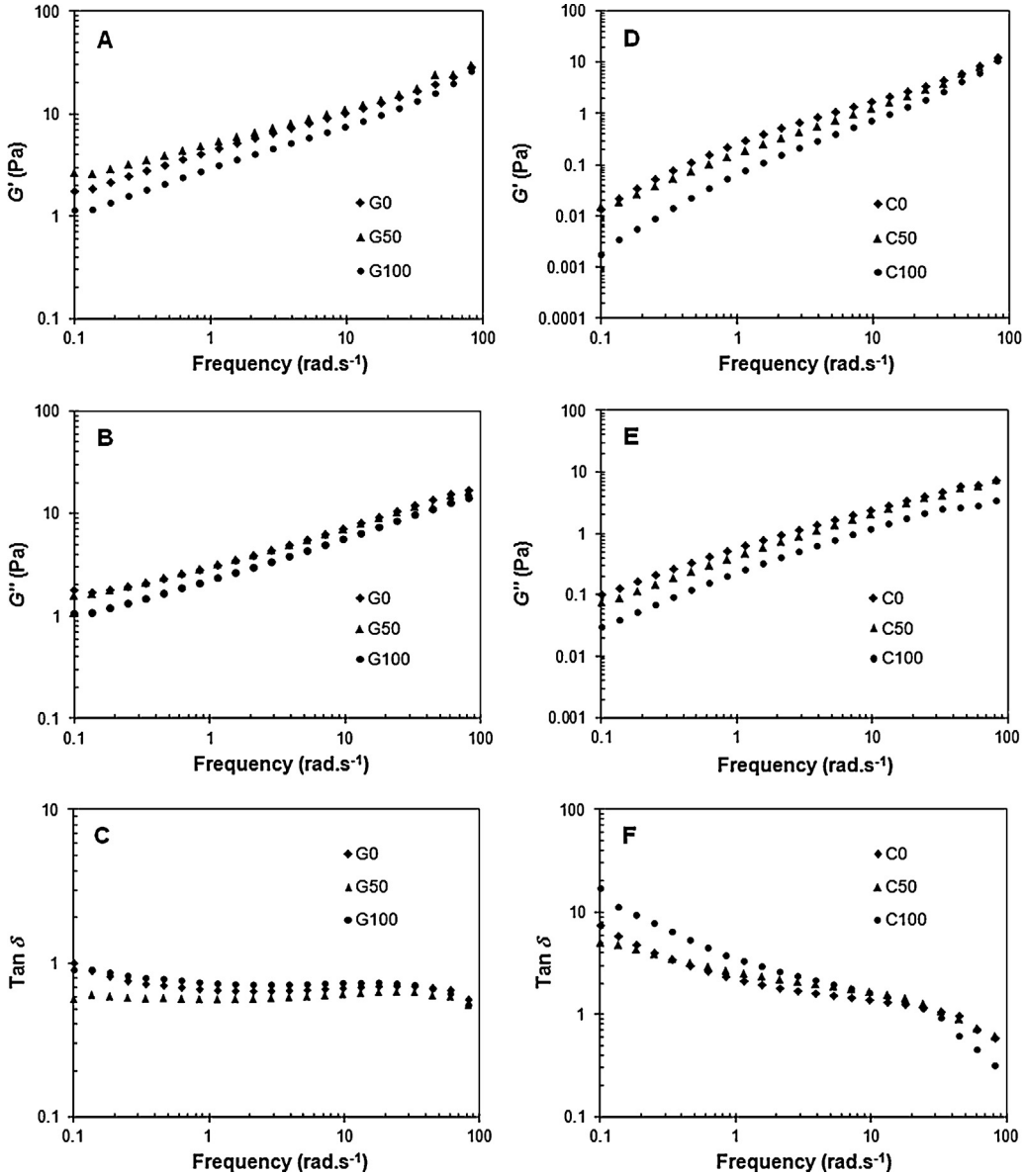

Fig. 4. Storage moduli (G'), loss moduli (G''), and loss tangents (tan δ) as a function of frequency of the 6% (w/w) untreated (G0, C0) and plasma-treated starch pastes at 50 W (G50, C50) and 100 W (G100, C100) measued at 1 Pa stress for granular samples (A–C) and 0.3 Pa for cooked samples (D–F). All measurements were performed at 25 °C.

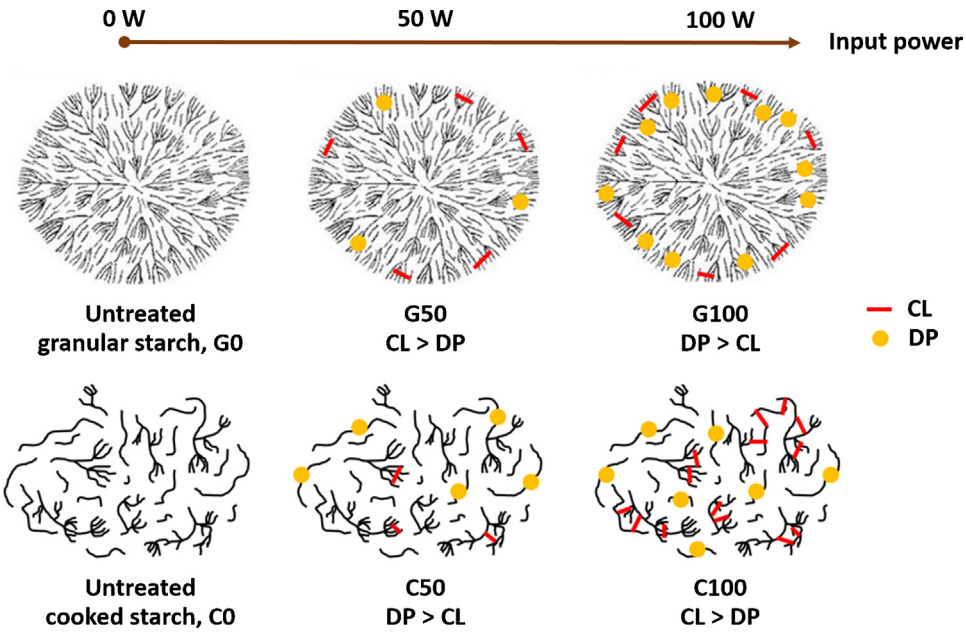

Fig. 5. Schematic diagram of proposed mechanisms of starch modification during jet atmospheric argon plasma treatment: CL, cross-linking and DP, depolymerization.

Table 3
Relative areas of relevant peaks of the untreated and plasma-treated starches measured using FTIR and ^{1}H NMR.

Sample[a]	Relative area	
	C—O—C peak (from FTIR)	OH peak (from ^{1}H NMR)
G0	0.34 ± 0.01	1.01 ± 0.02
G50	0.39 ± 0.05	0.97 ± 0.00
G100	0.25 ± 0.04	1.06 ± 0.04
C0	0.31 ± 0.01	1.03 ± 0.07
C50	0.25 ± 0.02	1.06 ± 0.02
C100	0.34 ± 0.01	1.00 ± 0.07

[a] Refer to Table 2 for the sample codes.

For steady shear test of the C samples, all the pastes showed totally different behavior from the G samples. Strong anti-thixotropy was observed in the first cycle of shear ramping in the steady flow test (data not shown), which similar to that of waxy maize starch (Wang, Li, Wang, & Ozkan, 2010). Such behavior was proposed to be a result from the formation of amylopectin complex structure during shearing. Again, the data of shear ramping of the second cycle, however, was almost identical to that of the shear ramping down of the first cycle and showed non-thixotropic behavior. Therefore, the data of shear stress and shear rate of shear ramping up of the second cycle was used to characterize the flow behavior of the samples using power law equation as shown in Table 2. In the case of C samples, the *K* values decreased after plasma treatment and the C100 sample exhibited lower *K* value than the C50 sample. These results are consistent with the dynamic modulus results observed at low frequencies (Fig. 4D and E).

3.6. Fourier transform infrared (FTIR) spectroscopy

The FTIR band at 1149 cm^{-1} was referred to C—O—C asymmetric stretching glycosidic bond and the band at 924 cm^{-1} was corresponded to C—O—C skeletal mode of α-glycosidic linkage (Deeyai et al., 2013). The relative areas of these peaks against the standard peak of KSCN at 2052 cm^{-1} indicated the occurrence of C—O—C bonding. The G50 and C100 exhibited higher relative areas of C—O—C than their control counterparts (Table 3), signifying that the predominant cross-linking occurred as evidenced by an increase in glycosidic linkage via plasma treatment. A mechanism of plasma-induced cross-linking was proposed as follows (Zou et al., 2004):

$$\text{Starch—OH} + \text{HO—Starch} \rightarrow \text{Starch—O—Starch} + H_2O \quad (3)$$

This mechanism forces one O—H bond and one C—OH bond to break before cross-linking to a new C—O—C glycosidic bond between two starch chains and abstracting one water molecule. On the other hand, the lower relative intensities of C—O—C were found in the G100 and C50 samples compared to their control ones (Table 3). Depolymerization might dominantly occur by cleaving C—O—C glycosidic bonds of starch molecules. The relative areas of the plasma-treated samples were slightly different from that of the untreated starch samples, indicating that mild modifications, i.e. giving slightly cross-linked or depolymerized starch, were attained.

3.7. ^{1}H nuclear magnetic resonance (^{1}H NMR)

The area of peak belonging to OH-group protons at chemical shift of 5.0 ppm was calculated as relative intensity against peak at chemical shift of 4.5 ppm which referred to H-4, H-5 in glucose units of starch molecules. The H-4, H-5 peak was considered to be unchanged during either cross-linking or depolymerization and thus this peak was used as an internal reference for calculation of the relative intensity of OH-group protons. The ^{1}H NMR analysis showed that the relative intensity of OH-group protons decreased for the G50 and C100 samples as compared with their controls (Table 3), indicating the loss of OH groups in the modified starch probably due to the predominant cross-linking reaction. It also showed that the relative intensity of OH-group protons increased in the case of the G100 and C50 samples, because of the predominant effect of depolymerization. Zou et al. (2004) have modified starch using glow discharge argon plasma at below atmospheric pressure. These authors reported that the area of peak belonging to OH-group protons decreased, indicating the loss of OH groups in the modified starch. These results revealed that the cross-linking took place and one molecule of water was split from two OH groups of starch chains as presented by Eq. (3). Similar to FTIR results, the relative areas of untreated and plasma-treated samples were slightly

different. Such observation confirmed that slightly cross-linked or depolymerized starch was obtained from the treatments.

3.8. Proposed mechanisms of starch modification by argon plasma treatment

According to a series of analytical results as explained above, the proposed mechanisms of starch modification during jet argon plasma treatment under atmospheric pressure can be drawn as shown in Fig. 5. For the cooked starch, the semi-crystalline structure of starch granules is totally destroyed by heat, causing amylose and amylopectin chains well dispersed in the slurry system. In our case, we have found that the C100 condition had undergone cross-linking more frequent than the C50 condition. The cross-linking mechanism requires one O—H bond and one C—OH bond to be broken before forming a new C—O—C glycosidic bond between two starch chains and abstracting one water molecule. In general, it is known that the bond energy is in the following order; O—H > C—H > C—O (Cottrell, 1958). The 100-W condition generated relatively more energetic particles to break the stronger O—H bonds. Also, under the 100-W condition all particles were generated more frequently than the 50-W condition. These two facts or the synergy between them have caused the well-dispersed cooked starch at 100 W, namely, C100 to be more readily to cross-link than the C50 condition. The lack of such under C50 condition caused a difficulty to form cross-linking but a preference to break C—O bonds, leading to the greater degree of depolymerization. For the granular starch, the structure of starch granules is still intact during plasma treatment, in which amylose and amylopectin chains are closely packed within the granules. In the case of granular form, only starch molecules on the granular surface could be exposed to plasma. The mobility of starch molecules in the granules is rather more restricted. This has become an additional complication, which may lead to suppression of depolymerization, especially, under the 50-W condition. Under the G100 condition, higher fragmentation of starch molecules may be expected due to higher plasma intensity. This may thus enhance depolymerization. Therefore, sample preparation and input power played essential roles to determine which competitive reactions to be dominant.

4. Conclusions

Non-chemical argon plasma treatment at atmospheric pressure is an alternative to typical chemical modification of starch. Two competitive reactions, i.e. cross-linking and depolymerization of starch, occurred during plasma treatment. The predominant effect of these two reactions was determined by the preparation of starch slurry and the input power to plasma treatment. The treatment of cooked starch at 100 W and granular starch at 50 W induced predominantly cross-linking rather than depolymerization. On the contrary, depolymerization predominated cross-linking for the treatment of cooked starch at 50 W and granular starch at 100 W. However, the drawbacks of this technique were the reactions induced by plasma can only take place on the surface of materials and cannot penetrate deeply into the starch slurry. Limitation of large volume treatment of jet plasma was also found. We might obtain only slightly cross-linked or depolymerized starch using this technique. These plasma-modified starches, i.e. cross-linked starch and depolymerized starch, can replace conventional chemically modified starches, i.e. chemically cross-linked starch and chemically depolymerized (such as acid-thinned) starch, respectively, used as main or minor ingredients in food products and promote new healthy food products. Further study for scaling up a plasma reactor for better modification and higher throughput of modified starch is underway.

Acknowledgements

The authors gratefully thank National Research Council of Thailand and National Science and Technology Development Agency for financial support. Panakamol Deeyai acknowledges the Commission for Higher Education, Ministry of Education for the scholarship. Siam Modified Starch Co. Ltd. (Pathum Thani, Thailand) is acknowledged for providing tapioca starch used in this study. We also thank the Department of Chemistry, Faculty of Science, Mahidol University and Central Instrument Facilities (CIF) Unit, Mahidol University, Kanchanaburi Campus for providing the NMR instrument and relevant equipment, respectively. Finally, we acknowledge Prof. Mudtorlep Nisoa and his laboratory for providing plasma equipment and Ms. Thidarat Makmoon for technical assistance in rheological measurement.

References

Bello-Pérez, L. A., Romero-Manilla, R., & Paredes-López, O. (2000). Preparation and properties of physically modified banana starch prepared by alcoholic-alkaline treatment. *Starch/Stärke*, *52*, 154–159.

Bogaerts, A., Neyts, E., Gijbels, R., & Van der Mullen, J. (2002). Gas discharge plasmas and their applications. *Spectrochimica Acta Part B: Atomic Spectroscopy*, *57*, 609–658.

Carmona-Garcia, R., Sanchez-Rivera, M. M., Méndez-Montealvo, G., Garza-Montoya, B., & Bello-Pérez, L. A. (2009). Effect of the cross-linked reagent type on some morphological, physicochemical and functional characteristics of banana starch (*Musa paradisiaca*). *Carbohydrate Polymers*, *76*, 117–122.

Chatakanonda, P., Varavinit, S., & Chinachoti, P. (2000). Effect of crosslinking on thermal and microscopic transitions of rice starch. *LWT-Food Science and Technology*, *33*, 276–284.

Cheng, H. N., & Neiss, T. G. (2012). Solution NMR spectroscopy of food polysaccharides – Reviews. *Polymer Reviews*, *52*, 81–114.

Choi, S.-G., & Kerr, W. L. (2004). Swelling characteristics of native and chemically modified wheat starches as a function of heating temperature and time. *Starch/Stärke*, *56*, 181–189.

Cooke, D., & Gidley, M. J. (1992). Loss of crystalline and molecular order during starch gelatinization: Origin of the enthalpic transition. *Carbohydrate Research*, *227*, 103–112.

Cottrell, T. L. (1958). *The strengths of chemical bonds* (2nd ed.). London: Butterworths.

Craig, S. A. S., Maningat, C. C., Seib, P. A., & Hoseney, R. C. (1989). Starch paste clarity. *Cereal Chemistry*, *66*, 173–182.

Davis, W. M., Erickson, C. L., Johnston, C. T., Delfino, J. J., & Porter, J. E. (1999). Quantitative Fourier transform infrared spectroscopic investigation of human substance functional group composition. *Chemosphere*, *38*, 2913–2928.

Deeyai, P., Jitsomboonmit, P., Soonthonchaikul, W., Suphantharika, M., & Dangtip, S. (2010). Effect of atmospheric argon plasma on morphology of tapioca starch granule. *Journal of the Microscopy Society of Thailand*, *24*, 112–116.

Deeyai, P., Suphantharika, M., Wongsagonsup, R., & Dangtip, S. (2013). Characterization of modified tapioca starch in atmospheric argon plasma under diverse humidity by FTIR spectroscopy. *Chinese Physics Letters*, *30*, 018103-1–018103-4.

Dragunski, D. C., & Pawlicka, A. (2001). Preparation and characterization of starch grafted with toluene poly (propylene oxide) diisocyanate. *Materials Research*, *4*, 77–81.

Dutta, H., Paul, S. K., Kalita, D., & Mahanta, C. L. (2011). Effect of acid concentration and treatment time on acid-alcohol modified jackfruit seed starch properties. *Food Chemistry*, *128*, 284–291.

Jyothi, A. N., Moorthy, S. N., & Rajasekharan, K. N. (2006). Effect of cross-linking with epichlorohydrin on the properties of cassava (*Manihot esculenta* Crantz) starch. *Starch/Stärke*, *58*, 292–299.

Kaur, L., Singh, J., & Singh, N. (2006). Effect of cross-linking on some properties of potato starches. *Journal of the Science of Food and Agriculture*, *86*, 1945–1954.

Kerr, R. W., & Cleveland, F. C. Jr. (1959). Orthophosphate esters of starch. U.S. Patent No. 2,884,413.

Khondkar, D., Tester, R. F., Hudson, N., Karkalas, J., & Morrow, J. (2007). Rheological behavior of uncross-linked and cross-linked gelatinised waxy maize starch with pectin gels. *Food Hydrocolloids*, *21*, 1296–1301.

Koo, S. H., Lee, K. K., & Lee, H. G. (2010). Effect of cross-linking on the physicochemical and physiological properties of corn starch. *Food Hydrocolloids*, *24*, 619–625.

Lawal, O. S. (2004). Composition, physicochemical properties and retrogradation characteristics of native, oxidized, acetylated and acid-thinned new cocoyam (*Xanthosoma sagittifolium*) starch. *Food Chemistry*, *87*, 205–218.

Lii, C., Liao, C., Stobinski, L., & Tomasik, P. (2002a). Behaviour of granular starches in low-pressure glow plasma. *Carbohydrate Polymers*, *49*, 499–507.

Lii, C., Liao, C., Stobinski, L., & Tomasik, P. (2002b). Effects of hydrogen, oxygen, and ammonia low-pressure glow plasma on granular starches. *Carbohydrate Polymers*, *49*, 449–456.

Lii, C., Liao, C., Stobinski, L., & Tomasik, P. (2002c). Exposure of granular starches to low-pressure glow ethylene plasma. *European Polymer Journal*, *38*, 1601–1606.

Lim, S., & Seib, P. A. (1993). Preparation and pasting properties of wheat and corn starch phosphates. *Cereal Chemistry*, *70*, 137–144.
Liu, H., Chaudhary, D., Yusa, S., & Tadé, M. O. (2011). Glycerol/starch/Na^+-montmorillonite nanocomposites: A XRD, FTIR, DSC and ^1H NMR study. *Carbohydrate Polymers*, *83*, 1591–1597.
López, O. V., Zaritzky, N. E., & García, M. A. (2010). Physicochemical characterization of chemically modified corn starches related to rheological behavior, retrogradation and film forming capacity. *Journal of Food Engineering*, *100*, 160–168.
Okazaki, S., Kogoma, M., Uehara, M., & Kimura, Y. (1993). Appearance of stable glow discharge in air, argon, oxygen, and nitrogen at atmospheric pressure using a 50 Hz source. *Journal of Physics D: Applied Physics*, *26*, 889–892.
Pashkuleva, I., Marques, A. P., Vaz, F., & Reis, R. L. (2010). Surface modification of starch based biomaterials by oxygen plasma or UV-irradiation. *Journal of Materials Science: Materials in Medicine*, *21*, 21–32.
Raizer, Y. P. (1991). *Gas discharge physics*. Berlin: Springer-Verlag.
Reddy, I., & Seib, P. A. (2000). Modified waxy wheat starch compared to modified waxy corn starch. *Journal of Cereal Science*, *31*, 25–39.
Rutenberg, M. W., & Solarek, D. (1984). Starch derivatives: Production and uses. In R. L. Whistler, & E. F. Paschall (Eds.), *Starch: Chemistry and technology* (2nd ed., pp. 311–388). New York: Academic Press.
Sandhu, K. S., Singh, N., & Lim, S.-T. (2007). A comparison of native and acid thinned normal and waxy corn starches: Physicochemical, thermal, morphological and pasting properties. *LWT-Food Science and Technology*, *40*, 1527–1536.
Singh, A. V., & Nath, L. K. (2012). Synthesis and evaluation of physicochemical properties of cross-linked sago starch. *International Journal of Biological Macromolecules*, *50*, 14–18.
Szymanowski, H., Kaczmarek, M., Gazicki-Lipman, M., Klimek, L., & Woźniak, B. (2005). New biodegradable material based on RF plasma modified starch. *Surface & Coatings Technology*, *200*, 539–543.
Wang, B., Li, D., Wang, L., & Ozkan, N. (2010). Anti-thixotropic properties of waxy maize starch dispersion with different pasting conditions. *Carbohydrate Polymers*, *79*, 1130–1139.
Yeh, A. I., & Yeh, S. L. (1993). Property differences between cross-linked and hydroxypropylated rice starches. *Cereal Chemistry*, *70*, 596–601.
Yoneya, T., Ishibashi, K., Hironaka, K., & Yamanoto, K. (2003). Influence of cross-linked potato starch treated with $POCl_3$ on DSC, rheological properties and granule size. *Carbohydrate Polymers*, *53*, 447–457.
Zou, J.-J., Liu, C.-J., & Eliasson, B. (2004). Modification of starch by glow discharge plasma. *Carbohydrate Polymers*, *55*, 23–26.